

MOLECULAR DYNAMICS SIMULATION STUDY ON THE STRUCTURAL EVOLUTION OF LIQUID NICKEL NANOPARTICLES DURING RAPID COOLING

Cem Canan^{1,*}, Murat Celtek², Unal Domekeli³

¹Edirne Vocational College of Technical Science, Trakya University, 22030, Edirne – Türkiye

²Faculty of Education, Trakya University, 22030, Edirne – Türkiye

³Dept. of Physics, Trakya University, 22030, Edirne – Türkiye

*Corresponding author: cemcanan@trakya.edu.tr

Abstract

Due to their critical importance for science and technology, metallic nanoparticles have become the focus of many researchers in recent years. Thanks to their unique physical and chemical properties, they have many applications, ranging from mechanics and magnetics to optoelectronics and medicine. Nano-scale solidification is a crucial stage in additive manufacturing technology, as it influences the microstructure and performance of the finished product. In this work, we have studied in detail the microstructural evolution of a liquid nickel (Ni) nanoparticle consisting of 10192 atoms during its rapid cooling using molecular dynamics (MD) simulations. The solidification points of Ni nanoparticles were estimated for different cooling rates from the change in potential energy of the system during the rapid cooling process. The microstructural evolution was analyzed in detail using pair distribution functions (PDFs), Honeycutt–Andersen (HA) pair analyses, and atomic configuration images. The results show that the cooling rate has a profound effect on the micro-structure of the solidified Ni nanoparticle. While liquid Ni nanoparticle tend to form a crystalline phase when cooled at cooling rates of 0.1, 0.5 and 1.0 K/ps, the system tends to form a glassy structure at cooling rate of 20.0 K/ps.

Keywords: Ni nanoparticle, MD simulations, solidification, HA pair analyses, glassy structure.

INTRODUCTION

Metallic nanoparticles (MNPs) hold an important place in the field of nanoscience and nanotechnology due to their interesting physical and chemical properties that are quite different from their bulk forms [1-3]. Nano-scale solidification is a crucial step in additive manufacturing technology as it affects the microstructure and performance of the final product [4]. Solidification from the liquid is the preferred technique for preparing MNPs. The properties of a material depend on its microstructure, enabling the production of metallic materials with exceptional properties. Therefore, it is crucial to understand the microstructural evolution of MNPs during the solidification process [5]. The crystallization process that occurs during the transition from the liquid to the solid state was studied using various experimental methods [6–9]. However, due to various factors involved in homogeneous nucleation, it is difficult to analyze the nucleation process during crystallization using experimental methods, and only limited information can be obtained. On the other hand, MD simulations are a powerful method for monitoring atomic motions during phase transitions, allowing one to study metal cooling at a rate not possible with experimental techniques. Therefore, there are many MD simulation studies on the solidification processes of MNPs in the [3,5,10-13].literature For example, Samanteray et al. [5] investigated the microstructural evolution of metal nanoclusters

during the solidification process subjecting them to different cooling rates using MD simulation. They reported that the cooling rate profoundly affects the structure of the solidified nanoclusters. Agudelo et al. [3] examined the size effect on the solidification process of Ni nanoparticles using MD simulation. They observed that the solidification temperature increased with increasing particle size. In this study, we performed MD simulation with Sutton-Chen (SC) potential to investigate the effects of rate on the micro-structural properties and solidification and glass transition temperatures of the system during the rapid cooling process of liquid Ni NP.

EXPOSITION

In this study, the quantum Sutton-Chen (Q-SC) potential, which was reparametrized based on the Sutton-Chen (SC) potential by Cagin et al. [14], was used to describe the interactions between Ni-Ni in MD simulations. According to the Q-SC model, the total energy, *E*, of a system of *N* atoms can be written as follows [15]:

$$E_{tot} = \sum_{i} E_{i},\tag{1}$$

$$E_i = \sum_i \varepsilon \left[\sum_{j \neq i} \frac{1}{2} V(r_{ij}) - c \, \rho_i^{1/2} \right], \tag{2}$$

$$V(r_{ij}) = \left(\frac{a}{r_{ij}}\right)^n,\tag{3}$$

$$\rho_i = \sum_{j \neq i} \varphi(r_{ij}) = \sum_{j \neq i} \left(\frac{a}{r_{ij}}\right)^m. \tag{4}$$

where, r_{ij} is the distance between the atoms i and j, and $V(r_{ij})$ is the double potential energy between the atoms i and j representing repulsive interactions in total energy. ρ_i is the energy density function of the atom i, representing the attractive term in total energy. ε , ε , ε , ε , and ε are potential parameters. The values of these parameters calculated by Cagin et al. [14] for Ni are listed in Table 1.

Table 1. *Q-SC* potential parameters for Ni

Metal	ε (eV)	С	a (Å)	n	m
Ni	7.3767x10 ⁻³	84.745	3.5157	10	5

All simulations for spherical Ni NPs were performed in this study using the DLPOLY

parallel code simulation package [16]. The model NP used in the simulations had a diameter of 6 nm and number of atoms of 10192. The liquid Ni NP was formed using the following procedure: first, the NP was obtained by cutting it into a sphere from a face-centred cubic (fcc) crystal structure. The NP in the crystalline phase was then heated from 100 K to 1800 K at a rate of 0.5 K/ps. Finally, the NP was equilibrated at 1800 K for 100 ps to obtain a randomly distributed configuration in the liquid state. To observe the effect of the cooling rate on the solidification behavior of liquid Ni NPs, the system was cooled from 1800 K to 100 K at cooling rates of 0.1, 0.5, 1.0 and 20.0 K/ps, respectively. All MD simulations were using performed the NVT canonical ensemble. with periodic boundary conditions not applied to account for surface effects on the particle. The Leapfrog Verlet algorithm was used to solve the classical equation of motion with a time step of 1.0 fs. The desired temperature and ambient pressure were controlled by the Nose-Hoover thermostat [17] and the Berendsen [18] approximation, respectively.

The solidification temperature of a liquid NP can be estimated by monitoring temperature-dependent changes in the system's thermodynamic properties. The potential energy curves obtained from MD simulations for different cooling rates of liquid Ni NP are shown in Figure 1 in comparison with the heating curve.

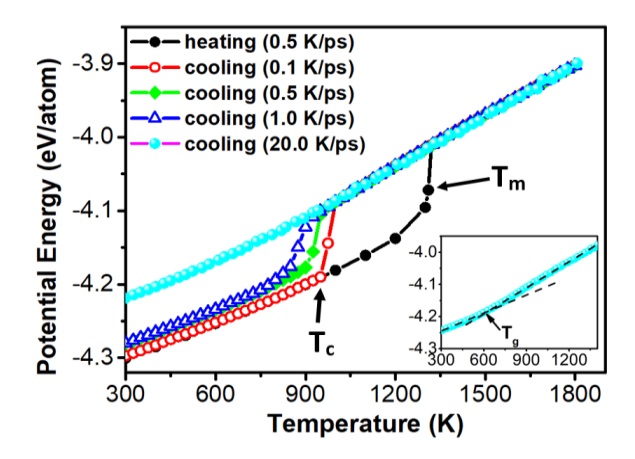


Fig. 1. Temperature-dependence of the potentials energy of Ni NP.

During the heating process, the potential energy increases linearly with temperature up to the melting temperature (T_m). At T_m, the system undergoes a first-order phase transition, resulting in a sudden change in the potential energy curve. In the liquid phase, the energy curve continues to increase linearly with temperature. During rapid cooling, the potential energy decreases linearly with decreasing temperature. A sudden decrease in potential energy occurs at cooling rates of 0.1 K/ps, 0.5 K/ps and 1.0 K/ps. This sudden decrease in the caloric curve is a clear indication that the system is transitioning from the liquid to the solid phase. As shown in Figure 1, the temperature at which this sudden decrease occurs is the solidification temperature (T_c) of the system. However, at a cooling rate of 20.0 K/ps, no sudden change in potential energy is observed; instead, there is a change in the slope of the energy curve. This behavior indicates that the system transforms into an amorphous (glassy) structure at a cooling rate of 20.0 K/ps. The glassy transition temperature (T_g) can be obtained by finding the intersection of the linear fit curves applied to the potential energy curve (see inset in Figure 1). The T_m, T_c and T_g values estimated from the energy curve for Ni NP are listed in Table 2. As the cooling rate increases, the T_c decreases.

Table 2. T_m , T_c and T_g values of Ni NP.

Rate	$T_m(K)$	$T_c(K)$	T _g (K)	
Heating 0.5 K/ps	1310			
Cooling 0.1 K/ps		950		
Cooling 0.5 K/ps		900		
Cooling 1.0 K/ps		850		
Cooling 20.0 K/ps			610	

The most effective method of obtaining information on the structural evolution of a liquid Ni NP during rapid cooling is to analyze the PDF, HA pair analysis and MD simulations snapshot in relation to temperature. The most straightforward method of determining whether a system is in a solid, liquid or glassy phase is to calculate the PDF. The PDF, g(r), can be calculated as follows [19]:

$$g(r) = \frac{\Omega}{N^2} \left\langle \sum_{i=1}^{N} \sum_{j\neq i}^{N} \delta(r - r_{ij}) \right\rangle, \tag{5}$$

where N and Ω represent the number of atoms, and volume of the simulations cell, respectively. Figure 2 shows the PDFs of liquid Ni NPs cooled at different rates at 300 K, compared with the PDF obtained from the heating process at the same temperature. The characteristic behavior of the PDF for at a cooling rate of 0.1 K/ps corresponds well with that of the ideal fcc crystal structure. As the cooling rate increases, the peak heights of the PDFs decrease, while their widths increase. The PDF continues to exhibit the characteristic behavior of an fcc-like crystal structure up to a cooling rate of 20.0 K/ps. However, the PDF of NP for a cooling rate of 20.0 K/ps clearly demonstrates that the system has a glassy structure due to the splitting observed in the second peak, which differs from the characteristic behavior of the liquid phase.

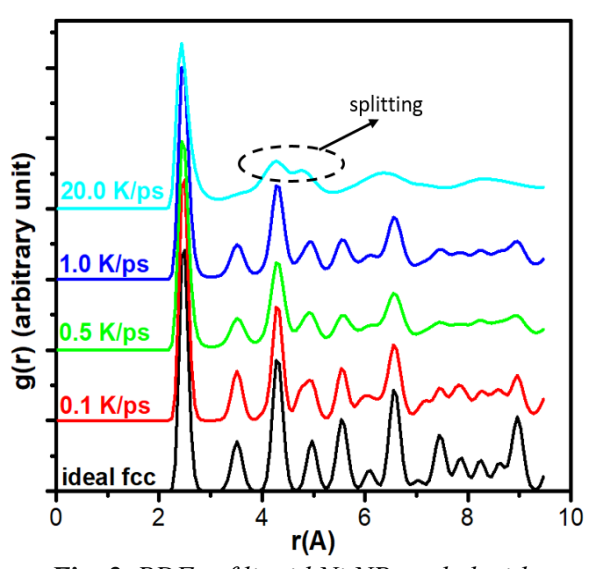


Fig. 2. PDFs of liquid Ni NP cooled with different cooling rates at T=300 K.

To understand the micro-structure of a system, the HA pair analysis technique can be used [13,20–22]. HA indices consist of four integers (i, j, k, and l), each serving a different function in defining the local structure. The first integer i is used to define the bond between two given atoms. If the root pairs are bonded, the first integer i is 1, otherwise it is 2. The second integer j is the

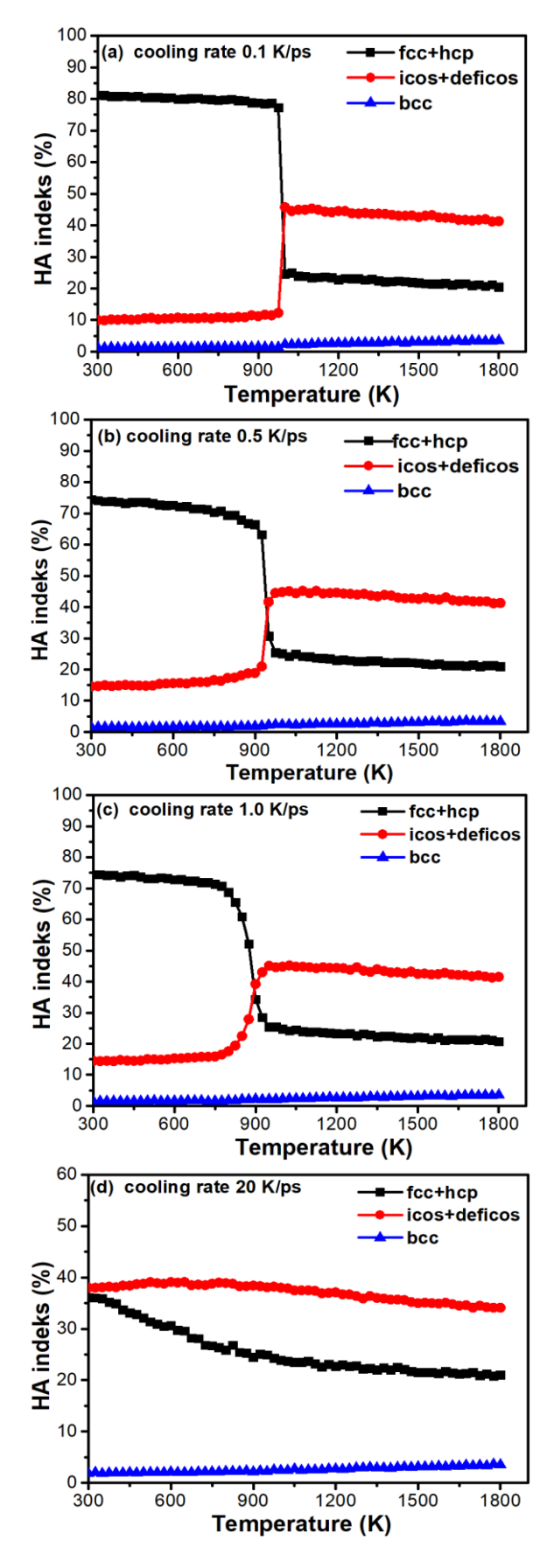


Fig. 3. Temperature dependent variation of the HA index of liquid Ni NP at various cooling rates.

number of adjacent neighboring atoms common to the root pairs, the third integer kis the number of close neighbor bonds between these common neighbors, and the fourth integer l is a parameter used to distinguish between local structures when i, j, and k are the same. In this work, bond type 1551 represents the ideal icosahedron (icos), and bond types 1541 and 1431 represent the defective icosahedron (deficos). The 1421 bond type is the characteristic bond type for the fcc crystal structure; the 1421+1422 bond types are the characteristic bond types representing the hexagonal close-packed hcp crystal structure, and the 1661+1441 bond types are the characteristic bond types representing the body-centered cubic (bcc) crystal structure. The total of bond types other than these is called other bond types. The temperature dependent change of HA indices calculated from MD simulation at different cooling rates for liquid Ni NP during the rapid cooling process is plotted in Figure 3. For cooling rates of 0.1 K/ps, 0.5 K/ps, and 1.0 K/ps, the percentage of HA index types changes abruptly at temperatures corresponding to T_c. Below T_c, percentage of fcc+hcp HA index types increases rapidly, while the percentage of icos+deficos HA index types decreases. Almost no change is observed in the percentage of bcc types during solidification period for each case. At 300 K, the percentage of fcc+hcp HA index types is higher than the other types for cooling rates of 0.1 K/ps, 0.5 K/ps, and 1.0 K/ps. Furthermore, as the cooling rate increases, the percentage of fcc+hcp types decreases, while the percentage of icos+deficos HA index types increases. For the cooling rates of 0.1 K/ps, 0.5 K/ps, and 1.0 K/ps, the percentages of fcc+hcp HA index types are 81%, 75%, and 74%, respectively. These results indicate that the liquid Ni NP transforms into a polycrystalline structure dominated by fcc crystal structures. The percentage of icos+deficos types in the system at 300 K is greater than the percentage of fcc+hcp types. The dominance of icos+deficos types, representing the

glassy structure, in the system is a clear indication that the liquid Ni NP transforms into a glassy structure. This result supports the PDF results.

Another way to gain insight into the structural changes of a system during the cooling process is to observe the snapshots obtained from the MD simulation. Snapshots of the liquid Ni NP at different temperatures for a cooling rate of 0.1 K/ps are shown in Figure 4. From 1800 K to 950 K, the atomic configuration exhibits a random atomic distribution, similar to that of a typical liquid system. At 950 K, an atomic configuration similar to that of a crystalline structure begins to form. This atomic order becomes more pronounced as the temperature decreases. At 300 K, it is clearly seen that the NP is in a crystalline phase.

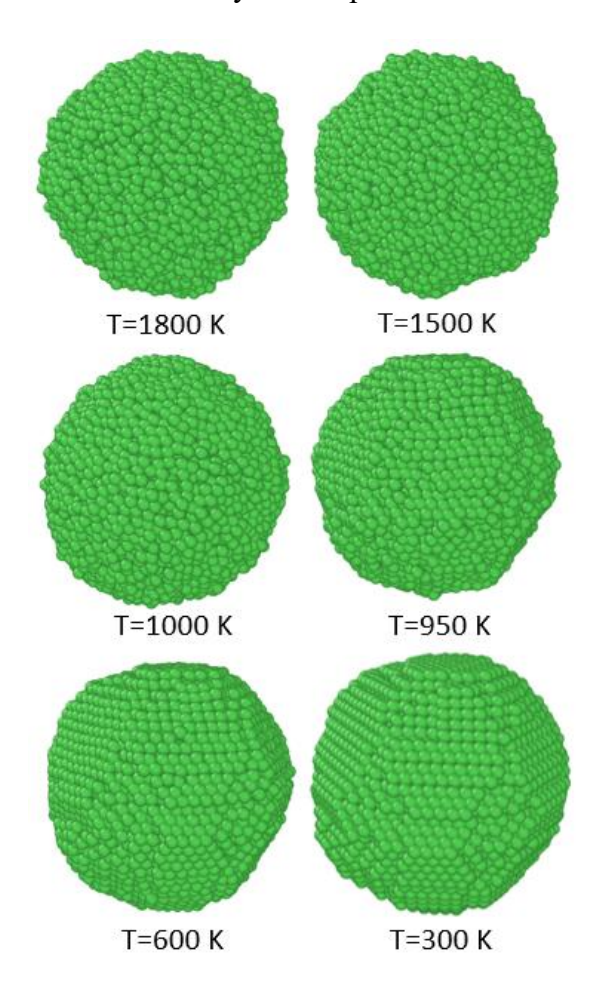


Fig. 4. Snapshots of liquid Ni NP at different temperatures for a cooling rate of 0.1 K/ps.

CONCLUSION

In this study, the effect of cooling rate on micro-structural changes solidification temperatures of liquid Ni NPs with a diameter of 6.0 nm and number of atoms 10192 during the rapid cooling process was investigated using simulation techniques. The results show that, from cooling rate of 0.1 K/ps to a critical cooling rate of 20.0 K/ps, the liquid Ni NP transforms into a polycrystalline structure dominated by the fcc crystal structure after cooling. At a critical cooling rate of 20.0 K/ps, the NP tends to form a glassy structure. Furthermore, the solidification temperatures of the system are directly related to the cooling rate. As the cooling rate increases, the solidification temperatures decrease. In summary, the cooling rate can be said to be an effective factor in the microstructural changes of liquid Ni NPs during solidification.

Funding No funding support has been received from any institution or person.

Acknowledgments: We would like to thank Trakya University Rectorate for giving permission and contributing to present this study as a paper.

REFERENCE

- [1] J. Mackerle, Nanomaterials, nanomechanics and finite elements: a bibliography (1994–2004), Model. Simul. Mater. Sci. Eng. 13 (2005) 123–158.
- [2] L. Deng, W. Hu, H. Deng, S. Xiao, Surface Segregation and Structural Features of Bimetallic Au–Pt Nanoparticles, J. Phys. Chem. C 114 (2010) 11026–11032.
- [3] J.D. Agudelo-Giraldo, D.F. Arias-Mateus, M.M. Gomez-Hermida, H. Reyes-Pineda, Structural analysis of Ni nanoparticles in thermal cooling by molecular dynamics, Bull. Mater. Sci. 46 (2023) 203.
- [4] J. D. Bernal, A Geometrical Approach to the Structure Of Liquids, Nat. Vol. 183 (1959) 141–147.

- [5] M.P. Samantaray, S.S. Sarangi, Effect of cooling rate on solidification points and atomic structures of metal nanoclusters: a molecular dynamics simulation study, Phys. Scr. 98 (2023) 125971.
- [6] F.J. Humphreys, The nucleation of recrystallization at second phase particles in deformed aluminium, Acta Metall. 25 (1977) 1323–1344.
- [7] S.P. Ringer, K. Hono, I.J. Polmear, T. Sakurai, Nucleation of precipitates in aged Al Cu Mg (Ag) alloys with high Cu:Mg ratios, Acta Mater. 44 (1996) 1883–1898.
- [8] P.-P.E.A. de Moor, T.P.M. Beelen, R.A. van Santen, In situ Observation of Nucleation and Crystal Growth in Zeolite Synthesis. A Small-Angle X-ray Scattering Investigation on Si-TPA-MFI, J. Phys. Chem. B 103 (1999) 1639–1650.
- [9] S.L. Price, Why don't we find more polymorphs?, Acta Crystallogr. Sect. B Struct. Sci. Cryst. Eng. Mater. 69 (2013) 313–328.
- [10] C. Gang, Z. Peng, L. Hongwei, Molecular Dynamics Simulation of Solidification of Pd-Ni Clusters with Different Nickel Content, Adv. Mater. Sci. Eng. 2014 (2014) 1–7.
- [11] Q. Bizot, O. Politano, V. Turlo, F. Baras, Molecular dynamics simulations of nanoscale solidification in the context of Ni additive manufacturing, Materialia 27 (2023) 101639.
- [12] Z.-A. Tian, R.-S. Liu, P. Peng, Z.-Y. Hou, H.-R. Liu, C.-X. Zheng, K.-J. Dong, A.-B. Yu, Freezing structures of free silver nanodroplets: A molecular dynamics simulation study, Phys. Lett. A 373 (2009) 1667–1671.
- [13] S.S. Murat Celtek, Unal Domekeli, The structural evolution of liqud Pb nanoparticle during solidification process, Int. Sci. Conf. UNITECH 2019 (2019) III-

- 335–339.
- [14] T. Çağin, Y. Kimura, Y. Qi, H. Li, H. Ikeda, W.L. Johnsonb, W.A. Goddard, Calculation of Mechanical, Thermodynamic and Transport Properties of Metallic Glass Formers, MRS Proc. 554 (1999) 43.
- [15] A.P. Sutton, J. Chen, Long-range Finnis—Sinclair potentials, Philos. Mag. Lett. 61 (1990) 139–146.
- [16] W. Smith, T.R. Forester, DL_POLY_2.0: A general-purpose parallel molecular dynamics simulation package, J. Mol. Graph. 14 (1996) 136–141.
- [17] S. Nose, A unified formulation of the constant temperature molecular dynamics methods, J. Chem. Phys. 81 (1984) 511–519.
- [18] H.J.C. Berendsen, J.P.M. Postma, W.F. van Gunsteren, A. DiNola, J.R. Haak, Molecular dynamics with coupling to an external bath, J. Chem. Phys. 81 (1984) 3684–3690.
- [19] U. Domekeli, M. Celtek, Melting mechanism of cylindrical molybdenum nanowire: a molecular dynamics simulation study, UNITECH 2024 Sel. Pap. (2024).
- [20] J.D. Honeycutt, H.C. Andersen, Molecular dynamics study of melting and freezing of small Lennard-Jones clusters, J. Phys. Chem. 91 (1987) 4950–4963.
- [21] U. Domekeli, A molecular dynamic study of the effects of high pressure on the structure formation of liquid metallic Ti₆₂Cu₃₈ alloy during rapid solidification, Comput. Mater. Sci. 187 (2021) 110089.
- [22] F.A. Celik, S. Kazanc, Crystallization analysis and determination of Avrami exponents of CuAlNi alloy by molecular dynamics simulation, Phys. B Condens. Matter 409 (2013) 63–70.